Article Summary Line: This work provides the rationale to consider electroceutical fabric generating weak potential difference of 0.5V, or other materials with comparable property, as material of choice for the development of PPE in the fight against COVID-19.

Running Title: Electroceutical Fabric for PPE against COVID-19

Keywords: personal protective equipment, nanoparticle, COVID-19.

Electroceutical Fabric Lowers Zeta Potential and Eradicates Coronavirus Infectivity upon Contact

Abhishek Sen[1], Dolly K Khona[1], Subhadip Ghatak[1], Vinoj Gopalakrishnan, Kenneth Cornetta, Sashwati Roy, Savita Khanna and Chandan K Sen[2]

Affiliations:

Indiana Center for Regenerative Medicine & Engineering at Indiana University School of Medicine, Indianapolis, Indiana, USA (A. Sen, D. K Khona, S. Ghatak, V. Gopalakrishnan, S. Roy, S. Khanna, C. K Sen)

Department of Medical and Molecular Genetics at Indiana University School of Medicine, Indianapolis, Indiana, USA (K. Cornetta)

[1] These first authors contributed equally to this article.

[2] **Corresponding Author:** Professor Chandan K. Sen

Indiana Center for Regenerative Medicine & Engineering,

Indiana University School of Medicine, Indianapolis, IN 46202

Tel: +1 317-278-2736; Fax: 317-278-2708

E-mail: cksen@iu.edu

Abstract

Coronavirus with intact infectivity attached to PPE surfaces pose significant threat to the spread of COVID-19. We tested the hypothesis that an electroceutical fabric, generating weak potential difference of 0.5V, disrupts the infectivity of coronavirus upon contact by destabilizing the electrokinetic properties of the virion. Respiratory coronavirus particles (10^5) were placed in direct contact with the fabric for 1 or 5 minutes. Viral particles ($2.5\text{-}4x10^4$) were recovered from the fabric. Following one minute of contact, zeta potential of the coronavirus was significantly lowered indicating destabilization of its electrokinetic properties. Size-distribution plot showed appearance of aggregation of the virus. Testing of the cytopathic effects of the virus showed eradication of infectivity as quantitatively assessed by PI-calcein and MTT cell viability tests. This work provides the rationale to consider the studied electroceutical fabric, or other materials with comparable property, as material of choice for the development of PPE in the fight against COVID-19.

The basic reproductive number of an infection, denoted as R_o, gauges the number of susceptible individual(s) that an infectious host can spread their disease to. While this epidemiological metric for severe acute respiratory syndrome (SARS) was reported to be 3 by the WHO, recent studies on COVID-19 estimates its R_o to be 5.7 making containment more challenging (*1*). Respiratory infections are known to spread through direct routes of aerosolization such as sneezing, coughing and other contact gestures. In addition, indirect modes of transmission play a significant role in determining R_o. SARS-CoV-2 remains viable for an extended period of time. The CDC reported presence of SARS-CoV-2 RNA on various surfaces on the Diamond Princess ship 17 days after all symptomatic and asymptomatic COVID-19 passengers had vacated (*2*,*3*). In a laboratory-based experimental study, SARS-CoV-2 remained viable for at least three hours in aerosols and up to 72 hours on fomites such as stainless steel (*4*). Use of personal protective equipment (PPE) is essential to safeguard healthcare providers against COVID-19 (*5*). However, use of these PPE itself poses significant threat as doffing of contaminated PPE carrying viable viral particles is likely to infect the person and potentially spread infection (*6*). Although CDC has recommended strict doffing procedures to reduce risk of nosocomial infections, contaminated PPE poses an imminent serious risk for healthcare professionals (*7*-*9*).

Infectivity of a viral particle is dependent on its stability. Multiple biophysical factors determine the stability of coronaviruses (*10*). For instance, nonspecific electrostatic interactions influence capsid assembly of enveloped RNA viruses in which positively charged capsid proteins package the negatively charged RNA. In positive-sense single-stranded RNA viruses, such as the coronaviruses, this thermodynamically spontaneous assembly is mediated by arginine rich motifs. A large number of ss-RNA-viruses follow a general law of packaging, based on

electrostatic forces without an explicit dependence on the sequence specificity (*11*). The overall positive charge of the capsid limits viral genome length (*12,13*). However, coronaviruses express an exoribonuclease associated with nonstructural protein 14 which allows them to inherit longer genomes when compared to other RNA viruses (*14*). Destabilization of coronavirus outside the host system is therefore of paramount importance in abating the spread of infection. We have co-developed a wireless electroceutical fabric for use as wound care dressing (*15-17*). This dressing, upon contact with bodily fluids or other aqueous wetting media, generates weak electric field which is effective in managing biofilm infection and improving wound healing (*16,18,19*). The dressing is currently FDA cleared and in clinical trial (NCT04079998). In this work we sought to investigate the effectiveness of the said electroceutical fabric for its ability to curb coronavirus infectivity.

Methods

Electroceutical Fabric

An FDA cleared wireless electroceutical dressing was used as a source of weak electric field for the current study and is referred to as electroceutical fabric (f_e). This fabric, co-developed by our laboratory (15-19), has been commercialized by Vomaris Inc. (Phoenix, AZ) was provided to us by the manufacturer. It is made of polyester fabric printed with alternating circular dots of Ag and Zn metals (ø2 mm and 1 mm, respectively), generating electric fields. A polyester fabric without any metal deposition (hence unable to generate electric field) was used as an experimental control and is referred to as sham fabric (f_s).

Viruses and Cell Lines

Respiratory coronavirus (ATCC® VR-2384™) and its host porcine cell line - ST (ATCC® CRL-1746™) were procured from ATCC. Lentivirus - CSCGW *mut6* [HIV-1-based vector expressing green fluorescent protein (GFP)] and cell line HEK293 used in this study were gifts from Prof. Kenneth Cornetta.

Cell Culture

Cell lines were cultured and maintained in respective cell culture medium at 37°C and humidified 5% CO_2 in air atmosphere. All culture media were made complete by addition of Fetal Bovine Serum (FBS, final concentration 10%, Sigma-Aldrich, F2442) and antibiotic-antimycotic solution (final concentration 1X; 15240-062, Life Technologies). For coronavirus studies, ST cells were cultured in complete Eagle's Minimum Essential Medium (EMEM, ATCC® 30-2003™). HEK293 cells were cultured in complete Dulbecco's Modified Eagle's Medium (DMEM, Cat no: 11995073, Gibco™).

Respiratory Coronavirus Infection and Propagation

ST cells were cultured in complete EMEM till they attained a confluency of 80-90% followed by washing monolayers with 5 ml of 1X PBS. Coronavirus stock (ATCC VR-2384; USDA permit 141794) aliquot was diluted with 3 ml of incomplete culture medium (without FBS and antibiotic-antimycotic solution) to attain a Multiplicity of Infection (MOI) of 1. This diluted viral stock was added to the washed monolayer and incubated at 37 °C, humidified 5% CO_2 in air atmosphere. Flasks were rocked gently for 2 min at intervals of 30 min, to re-distribute viral inoculum. After 2h infection, viral adsorption was terminated by adding 10 ml of complete culture medium to the monolayer.

Coronavirus Purification

Coronavirus purification was performed as described previously (*29*). In brief, culture medium from flasks with infected cells was harvested at 10000xg for 20 min at 4 °C. Viral precipitation from this supernatant (12 ml) was done by addition of polyethylene glycol and NaCl. PEG precipitated proteins and virions were pelleted at 10000xg for 30 min at 4°C and the pellet was dissolved in 100 µl of ice-cold 1X HEPES-saline buffer (10 mM HEPES – Sigma H7523 + 0.9% w/v NaCl, pH 6.7). Dissolved pellet was then loaded on a discontinuous sucrose gradient (10-20-30%, 800 µl each; in 1X HEPES-saline) and subjected to ultracentrifugation at 100000xg for 90 min at 4°C.

Nanoparticle Tracking Analysis

Viruses were diluted in EMEM or 18.2 MΩ water. Mean particle diameter and concentration of viral particles were analyzed by NanoSight NS300 with a 532 nm laser and SCMOS camera (Malvern) as previously described (*30,31*). Standard 100 nm latex spheres were run at 1000:1 dilution in milliQ to test optimal instrument performance. Data were analyzed using NTA 3.0 software (Malvern Instruments).

Zeta Potential Analysis

Zeta (ζ) potential measurement of viral particles was determined by Zetasizer (Nano-Z, Malvern Instruments Ltd., UK) as described previously (*30,31*). All samples were dispersed in double-distilled water and tested in volume-weighted size distribution mode in folded capillary cells (Fisher Scientific NC0491866). An average of three readings (60s) were recorded.

Scanning Electron Microscopy

Viral particles were suspended in ddH2O with 2.5% glutaraldehyde or other buffer and dropped onto clean silica wafers. After drying, samples were desiccated in a vacuum chamber for at least 12h before analysis. Images were obtained after carbon sputter coating using a field emission scanning electron microscope (JEOL 7800F, JEOL Japan) at a beam energy of 5 or 10 kV. For the SEM images of the fabric, gold sputter coating was used.

Energy Dispersive X-ray (EDX) Microanalysis

For elemental detection, the EDX microanalysis associated with SEM was used (*32*). The x-ray emissions at different wavelengths were measured using a photon-energy-sensitive detector. The EDX detector system performed a simultaneous display of all mid-energy (1-20 keV) x-rays collected during any individual analysis period.

Coronavirus and Lentivirus Infectivity

ST (coronavirus) and HEK 293 (lentivirus) cells were seeded at densities of 10,000 /well and 1000 /well in 24-well and 96-well cell culture plates, respectively. Seeded plates were incubated at 37°C, 5% CO_2 humidified incubator for 18h. One hundred microliter (10^5 particles) of aqueous suspension of viruses (10^6/ml of VR-2384 or CSCGW mut6 lentivirus) were placed on 1.5 cm diameter discs of f_e and f_s at room temperature and time was allowed for the droplet to be fully absorbed into the respective fabric. As soon as that was achieved, a timer was started for either 1 min or 5 min of contact time followed by recovery of the particles. Serum free medium (100µl) was used to rinse each fabric for recovering viral particles from the fabric. NTA was performed, as above, to estimate viral recovery efficiency. Recovered VR-2384 viruses were diluted with serum free medium and used to infect ST cells at MOI of 10 (10^5 viruses). Recovered CSCGW *mut6* virus was diluted in complete DMEM medium followed by HEK293 transduction at MOI of 10 (4×10^4 viruses). Parallel sets of cells infected with untreated viruses

(at the same MOI as that of treated viruses) were used as positive control while uninfected or non-transduced host cells were accounted as negative control. The expression of GFP in transduced HEK293 was assessed after 7 days to ascertain the effect of f_e treatment on lentiviral infectivity. Six technical replicates and twelve biological replicates were studied.

Cell Viability Staining by Calcein AM and Propidium Iodide

Viability of ST cells, infected as above, was assessed by dual staining with Calcein AM and Propidium iodide (PI) (*31*). Media from wells with ST cells (uninfected or infected with untreated or fabric-contacted viruses) was washed briefly with 1ml of 1X PBS (per well) for 1 min, followed by addition of 250µl of freshly-prepared staining solution in 1X PBS (Calcein AM; final concentration 1 µg/ml, Catalog no: C1430, Invitrogen™) and PI (Sigma-Aldrich). Cells were incubated under dark conditions at 37°C for 15 min and then observed under a Confocal Laser Scanning Microscope using a 10X objective. The ratio of PI:calcein signal was normalized with the average PI intensity of untreated cells to obtain fold-change compared to non-viable cells (basal cell death) in untreated cells.

Cell Viability Assessment by MTT Assay

Cell viability of ST cells infected as above was assayed using the MTT (3-(4,5-Dimethylthiazol-2-yl)-2,5-diphenyltetrazolium bromide) assay as per manufacturer's protocol (MTT assay kit, Catalog no: ab211091, Abcam).

Statistical Analysis

GraphPad Prism (GraphPad Software) v8.0 was used for statistical analyses. Statistical analysis between multiple groups were performed using one-way analysis of variance with the post-hoc Sidak multiple comparison test. Statistical analysis between two groups was performed

using unpaired Student's two-sided t tests. $P<0.05$ was considered statistically significant. Significance levels and exact P values are indicated in all relevant figures. Data were normally distributed. Data for independent experiments were presented as means ± SEM unless otherwise stated. Individual data points are plotted reflecting n (8-19) for each experiment.

Results

Characterization of the Electroceutical Fabric

The electroceutical fabric tested is made up of polyester fabric printed with alternating circular regions of Ag and Zn dots (Figure 1A). The Ag dots (ø 2mm) and Zn dots (ø 1mm) were printed on the fabric in proximity of about 1 mm to each other. Scanning electron microscopy (SEM) displayed the deposition of Ag particles and Zn on the fibers of the polyester fabric (Figure 1A). EDX microanalysis revealed the presence of Ag and Zn on the electroceutical fabric (f_e) and absence in the sham polyester fabric (f_s) (Figure 1B-C). The only peak that was present other than C and O was that of Au used for coating the fabrics for SEM imaging (Figure 1C). Proximity of Ag and Zn on polyester fabric forms a redox couple and is capable of driving electrochemistry when wet in an aqueous ionized environment including any body fluid (Figure 1D). Ag and Zn were spotted on another textile which was also appropriate for the preparation of stretchable facemasks (Figure 1E). SEM of the fabric used for such mask showed a different weaving pattern (Appendix Figure 1A-C). Deposition of Ag and Zn on the fabric for facemask was tested by EDX spectrum analysis (Appendix Figure 1B). Our primary line of investigation focused on the polyester-based electroceutical fabric (Figure 1A right). Three ionized aqueous media were used to test potential difference between adjacent Ag and Zn deposits. NaCl solution (0.85% w/v), cell culture medium and tap water (of practical value to end users of PPE) were

tested at room temperature. The potential difference between the two electrodes rapidly increased and achieved a steady state after the first 15s (Figure 2).

Physical Characterization of the Coronavirus

SEM (150,000x) revealed the morphological features of the CoV particle (Fig 3A). Following spotting on the silicon wafer, the purified virus was fixed and subsequently dehydrated. A thin (2-5nm) layer of carbon was sputtered on the sample to make the specimen conductive. The size of the virus ranged between 75-125nm. Nanoparticle tracking analysis (NTA) revealed poly-dispersed peak (Figure 3B). The electrokinetic property, as represented by the ζ potential, of the viral particles is a parameter that determines adsorption and stability of the particle in any given dispersant medium. For practical purposes, viral particles are expected to be suspended in water droplets either aerosolized or resting on a surface. The average ζ potential of four different preparation of CoV was determined to be -25.675 mV (Figure 3C). All four-preparation demonstrated comparable ζ potential distribution and phase shift (Figure 3D-E). The average electrophoretic mobility distribution was determined to be -2μmcm/Vs (Figure 3F)

Electroceutical Fabric Attenuated the ζ Potential of Coronavirus upon Contact

Quantification of the viral particles after spotting on f_e yielded 44.29% and 23.73% recovery from the fabric when exposed for 1 min or 5 min, respectively (Figure 4A). Nanoparticle tracking analysis demonstrated that unlike the purified CoV that showed a single peak around 75nm, the recovered CoV showed additional peaks suggesting aggregation of the viral particles upon contact with the fabric (Figure 4B). Analysis of ζ potential showed significant graded attenuation of this electrokinetic property upon contact with the f_e (Figure 4C). Such lowering of average ζ potential of CoV, applied and recovered from f_e, has been plotted

(Figure 4D). Unlike 1 min exposure to the f_e, 5 min exposure showed an appreciable difference in the phase plot of the viral particles (Figure 4E).

Loss of Coronavirus Infectivity upon Contact with Electroceutical Fabric

To assess changes in the infectivity of CoV following contact with the electroceutical fabric, a cytopathic assay was employed. Infected cells were monitored for appearance of cytopathic effects (CPE; cell rounding and sloughing) until post-infection day 7. Overt CPE was observed on day 7 in response to CoV infection (Figure 5B; Appendix Figure 2). Comparable CPE was noted in response to treatment of cells with CoV recovered from sham control fabric f_s (Figure 5C; Appendix Figure 2). In contrast, CoV recovered from f_e did not cause any CPE indicating loss of its infectivity (Figure 5D; Appendix Figure 2). Cells treated with fe-recovered CoV particles appeared as healthy as the uninfected cells (Figure 5A; Appendix Figure 2). Objective assessment of cell viability was performed using a calcein/PI fluorescence assay. Only live cells with intracellular esterase activity hydrolyze the acetoxymethyl ester in non-fluorescent Calcein AM converting it into green fluorescent Calcein. Dead cells or cells with damaged or compromised cell membranes include PI stain, which is otherwise impermeant to live cells. Fold-change increase in PI/Calcein signal as shown indicates loss of cell viability in response to infection. Infection of cells with CoV caused marked loss of cell viability (Figure 5B). Such cytopathic effect of CoV was completely absent once the virus was exposed to f_e (Figure 5 D-E). The sham fabric did not afford such protection (Figure 5C, E). The cytopathic effects of CoV and the protective effects of f_e (versus f_s) was corroborated by the standard MTT assay commonly used for testing cell viability (Figure 5F).

Electroceutical Fabric Eliminated Lentiviral Transduction Efficacy

The lentiviral pseudotype system is a standard laboratory tool to study the infectivity of viruses under conventional biosafety conditions (*20*). Lentivirus CSCGW *mut6*, upon successful transduction in HEK293 cells, results in GFP-expressing host cells. Mammalian cells were treated with purified lentivirus or the same virus subjected to contact with f_e or f_s for 1 or 5 min as indicated in the figure legend (Figure 6). Transduced cells were monitored microscopically to check the presence of GFP+ cells. Lentiviral exposure caused widespread infection of cells. Treatment of cells with virus recovered from sham fabric f_s caused comparable infection (Figure 6B). However, contact of virus with the electroceutical fabric f_e, even for one minute, eliminated lentiviral infectivity (Figure 6B)

Discussion

Previous work from our laboratory has established the effectiveness of electroceutical principles as an alternative to pharmacological approaches in managing planktonic microbial pathogens and complex polymicrobial biofilms (*16,18,19,21*). Viruses are known to rely on electrostatic interactions for optimal virion assembly and attachment (*10*). For instance, structural proteins in coronaviruses, negatively charged amino acid residues in the nucleocapsid facilitates assembly with the membrane protein (*22*). Additionally, the coronavirus envelope protein is known to generate ion conductive pores across membranes which are voltage dependent (*23*). Leveraging these viral characteristics to achieve viral inactivation remains largely unexplored and has been attempted in this work.

Electroceuticals have generated renewed interest in the health care industry (*24*). The fabric tested in this work consists of only silver and zinc dots on polyester fabric that forms a redox couple (*15*). Zeta potential of a particle determines its electrostatic interactions in particle dispersions and, as such, is an important determinant of the stability of viral particles. Contact of

CoV with the electroceutical fabric studied rapidly lowered the zeta potential demonstrating a direct effect of the fabric on the electrokinetic properties of the viral particle. Any change of zeta potential towards zero is viewed as increase in electrical instability of the particle. The observation that contact with the electroceutical fabric eliminates infectivity of the virus leads to the hypothesis that the observed lowering of zeta potential may have caused defects in the structural integrity of the virus. Study of changes in the capsid-RNA structure following exposure to the weak electric field generated by the fabric is thus warranted.

CoV is a nanoparticle. Nanoparticle tracking analysis determines the hydrodynamic diameter of the analyte by applying the Stokes–Einstein equation after measuring the Brownian motion of individual nanoparticle. NTA was utilized to estimate absolute viral particle number and size distribution in not only pure CoV but also in CoV recovered from the fabric. Observed changes in particle number and size distribution support the aforementioned hypothesis that exposure to the weak electric field causes damaging structural alterations to the virions. Cells in culture routinely display a small fraction of dead or dying cells. Cytopathic effects of viral infection are tested to examine whether exposure to the infectious particle adds to the basal cell death burden of the culture. Long-term observations, i.e. days versus hours, ensure the recording of the eventual fate of the affected cells. Reporting of short-term data alone, while sometimes may be encouraging with respect to effect of the intervention, may simply reflect results representing postponement of death from the insult and not a true rescue. In CPE studies of this work, cell rounding and sloughing were evident in day 4 post-infection. During this time, cells treated with virus pre-exposed to the electroceutical fabric closely resembled cells that were unchallenged by exposure to the virus. In standard cell culture, the growth medium is changed every other day to wash off floating dead cells and to replenish nutrition. Under conditions of

infection by virus, such frequent change of cell culture medium is not made. Cells grow in the same spent media until day 7 post-infection. Maintenance of cells without any change in culture media for seven days is expected to marginally increase basal cell death burden as shown.

Textiles evaluated for use in PPE such as masks are subject to specific FDA 510(k) requirements expecting stringent viral filtration tests to demonstrate 99.9% reduction of 1.1–$3.3x10^4$ plaque forming units of standard phiX174 bacteriophage. The phiX174 is widely used as a model organism because of it being a standardized test. However, it is important to note that unlike SAR-CoV-2 which is a RNA virus, phiX174 bacteriophage is a DNA virus with numerous contrasting physical, chemical as well as biological properties. Furthermore, this bacteriophage is much smaller in size than SAR-CoV-2. The non-enveloped icosahedral morphology of phiX174 are aerosolized with a mean particle size of 3.0 ± 0.3 μm (*25*). This is in direct contrast with the coronaviruses that cause diseases in animals and humans which are ~100 nm in diameter and are aerosolized as respiratory droplets with sizes ≥5μm (*26*,*27*). Importantly, phiX174 cannot infect mammalian cells. It infects and forms visible plaques on a lawn of *Escherichia coli* (Migula) Castellani and Chalmers strains. In the context of COVID-19 pandemic, this work studies the coronavirus and tests cytopathic effects on mammalian cells. Testing methods such as AATCC TM100 recommends a textile contact time of 24h for both enveloped and non-enveloped viruses. We report results on contact time that is much shorter and more relevant to PPE usage in the context of COVID-19.

This work presents first evidence demonstrating that the physical characteristic features of CoV may be exploited to render it non-infective following exposure to weak electric field generating electroceutical fabric. The observation that lentiviral infectivity is also eliminated following contact with the electroceutical fabric contributes to the rigor of our central finding.

Lowering of zeta potential of the CoV particles following exposure to the electroceutical fabric constitutes direct evidence supporting the contention that electrokinetic stability of the viral particle is weakened. Additional studies are necessary to characterize specific structural changes in response to exposure to the electroceutical fabric, and to connect such changes to loss of infectivity. In the meanwhile, this work provides evidence supporting the rationale to consider the studied electroceutical fabric, or other materials with similar property, as material of choice for the development of PPE in the fight against COVID-19.

Acknowledgments

We would like to acknowledge the Integrated Nanosystems Development Institute (INDI) for use of their JEOL 7800-f Field Emission Scanning Electron Microscope, which was awarded through NSF grant MRI-1229514.

Author Bio (first author only, unless there are only 2 authors)

Abhishek Sen is an experienced molecular biologist specializing in microbial systems and interested in studying host-pathogen interactions. He is currently pursuing his pre-doctoral research as a Visiting Research Associate at the Indiana University School of Medicine and is a University of Nottingham graduate in M.Sc. Applied Biomolecular Technology. **Footnotes (if applicable)**

[1]These authors contributed equally to this article.

[2] Corresponding author

References

1. Sanche S, Lin YT, Xu C, Romero-Severson E, Hengartner N and Ke R. High Contagiousness and Rapid Spread of Severe Acute Respiratory Syndrome Coronavirus 2. Emerg Infect Dis. 2020;26.
2. MOJICA A. CDC examination of COVID-19 on cruise ships found COVID-19 RNA on surfaces for 17 days.
3. Oliver D. Coronavirus genetic material stayed on surfaces for up to 17 days on Diamond Princess cruise, CDC says.
4. van Doremalen N, Bushmaker T, Morris DH, Holbrook MG, Gamble A, Williamson BN, et.al. Aerosol and Surface Stability of SARS-CoV-2 as Compared with SARS-CoV-1. N Engl J Med. 2020; 382:1564-1567.
5. Holland M, Zaloga DJ and Friderici CS. COVID-19 Personal Protective Equipment (PPE) for the emergency physician. Visual journal of emergency medicine. 2020;19:100740-100740.
6. Wang D, Hu B, Hu C, Zhu F, Liu X, Zhang J, et.al. Clinical Characteristics of 138 Hospitalized Patients With 2019 Novel Coronavirus-Infected Pneumonia in Wuhan, China. JAMA. 2020.
7. Administration OSHA.
8. CDC. Use Personal Protective Equipment (PPE) When Caring for Patients with Confirmed or Suspected COVID-19.
9. Young R. Knowing How to Remove PPE Is A Matter Of Life And Death, One ER Doctor Says.

10. Perlmutter JD and Hagan MF. Mechanisms of virus assembly. Annu Rev Phys Chem. 2015;66:217-39.
11. Forrey C and Muthukumar M. Electrostatics of capsid-induced viral RNA organization. J Chem Phys. 2009;131:105101.
12. Belyi VA and Muthukumar M. Electrostatic origin of the genome packing in viruses. Proc Natl Acad Sci U S A. 2006;103:17174-8.
13. Hu T, Zhang R and Shkovskii BI. Electrostatic theory of viral self-assembly. Physica a-Statistical Mechanics and Its Applications. 2008;387:3059-3064.
14. Minskaia E, Hertzig T, Gorbalenya AE, Campanacci V, Cambillau C, Canard B et.al. Discovery of an RNA virus 3'->5' exoribonuclease that is critically involved in coronavirus RNA synthesis. Proc Natl Acad Sci U S A. 2006;103:5108-13.
15. Banerjee J, Das Ghatak P, Roy S, Khanna S, Sequin EK, Bellman K, et.al. Improvement of human keratinocyte migration by a redox active bioelectric dressing. PLoS One. 2014;9:e89239.
16. Ghatak PD, Schlanger R, Ganesh K, Lambert L, Gordillo GM, Martinsek P et.al. A Wireless Electroceutical Dressing Lowers Cost of Negative Pressure Wound Therapy. Adv Wound Care (New Rochelle). 2015;4:302-311.
17. Vilkhu R, Thio WJ, Ghatak PD, Sen CK, Co AC and Kiourti A. Power Generation for Wearable Electronics: Designing Electrochemical Storage on Fabrics. IEEE Access. 2018;6:28945-28950.
18. Banerjee J, Das Ghatak P, Roy S, Khanna S, Hemann C, Deng B, et.al. Silver-zinc redox-coupled electroceutical wound dressing disrupts bacterial biofilm. PLoS One. 2015;10:e0119531.

19. Barki KG, Das A, Dixith S, Ghatak PD, Mathew-Steiner S, Schwab E, et.al. Electric Field Based Dressing Disrupts Mixed-Species Bacterial Biofilm Infection and Restores Functional Wound Healing. Ann Surg. 2019;269:756-766.

20. Wang J, Deng F, Ye G, Dong W, Zheng A, He Q et.al. Comparison of lentiviruses pseudotyped with S proteins from coronaviruses and cell tropisms of porcine coronaviruses. Virol Sin. 2016;31:49-56.

21. Roy S, Prakash S, Mathew-Steiner SS, Das Ghatak P, Lochab V, Jones TH, et.al. Disposable Patterned Electroceutical Dressing (PED-10) Is Safe for Treatment of Open Clinical Chronic Wounds. Advances in wound care. 2019;8:149-159.

22. Kuo L and Masters PS. Genetic evidence for a structural interaction between the carboxy termini of the membrane and nucleocapsid proteins of mouse hepatitis virus. J Virol. 2002;76:4987-99.

23. Verdia-Baguena C, Nieto-Torres JL, Alcaraz A, DeDiego ML, Torres J, Aguilella VM et.al. Coronavirus E protein forms ion channels with functionally and structurally-involved membrane lipids. Virology. 2012;432:485-94.

24. Reardon S. Electroceuticals spark interest. Nature. 2014;511:18.

25. Rengasamy S, Shaffer R, Williams B and Smit S. A comparison of facemask and respirator filtration test methods. Journal of occupational and environmental hygiene. 2017;14:92-103.

26. Shiu EYC, Leung NHL and Cowling BJ. Controversy around airborne versus droplet transmission of respiratory viruses: implication for infection prevention. Curr Opin Infect Dis. 2019;32:372-379.

27. Tellier R, Li Y, Cowling BJ and Tang JW. Recognition of aerosol transmission of infectious agents: a commentary. BMC Infect Dis. 2019;19:101.
28. Brockmeier SL, Loving CL, Nicholson TL and Palmer MV. Coinfection of pigs with porcine respiratory coronavirus and Bordetella bronchiseptica. Vet Microbiol. 2008;128:36-47.
29. Maier HJ, Bickerton E and Britton P. Coronaviruses Methods and Protocols Preface. Coronaviruses: Methods and Protocols. 2015;1282:V-V.
30. Li J, Ghatak S, El Masry MS, Das A, Liu Y, Roy S, et.al. Topical Lyophilized Targeted Lipid Nanoparticles in the Restoration of Skin Barrier Function following Burn Wound. Mol Ther. 2018;26:2178-2188.
31. Ghatak S, Li J, Chan YC, Gnyawali SC, Steen E, Yung BC, et.al. AntihypoxamiR functionalized gramicidin lipid nanoparticles rescue against ischemic memory improving cutaneous wound healing. Nanomedicine. 2016;12:1827-1831.
32. Scimeca M, Orlandi A, Terrenato I, Bischetti S and Bonanno E. Assessment of metal contaminants in non-small cell lung cancer by EDX microanalysis. European journal of histochemistry : EJH. 2014;58:2403-2403.
33. Chan LL, McCulley KJ and Kessel SL. Assessment of Cell Viability with Single-, Dual-, and Multi-Staining Methods Using Image Cytometry. Methods Mol Biol. 2017;1601:27-41.

Address for Correspondence:

Chandan K. Sen, Indiana Center for Regenerative Medicine & Engineering, Indiana University School of Medicine, Indianapolis, IN 46202, USA; email: cksen@iu.edu Tel: +1 317-278-2736; Fax:317- 278-2708; E-mail: cksen@iu.edu

FIGURE LEGENDS

Figure 1: Physical characterization of fabrics. (**A**) Photomicrographs of sham fabric (f_s) and electroceutical fabric (f_e). SEM images of both fabrics were captured at 60X, 100X and 330X magnifications. Regions of silver and zinc metal deposition in f_e have been marked with red squares. (**B)** Energy Dispersive X-Ray (EDX) microanalysis of silver and zinc metal deposition on f_e. The gold peak in both spectra is from the gold sputter used to make the surface conductive prior to SEM. (**C**) EDX analysis of f_s. (**D**) f_e voltage measurement using a multimeter (Amprobe 34XR-A, Everett, WA). (**E)** Prototype face-mask developed using stretchable electroceutical textile.

Figure 2: The electroceutical fabric. Voltage generated by electroceutical fabric was measured using the Amprobe multimeter in three different aqueous wetting solutions: (**A**) NaCl (0.85% w/v); (**B**) Incomplete EMEM, and (**C**) Tap water. DC voltage was measured as shown. Probes were placed adjacent Ag and Zn dots and at 0s, 100 microliters of the respective wetting solution was added to the electroceutical fabric. Three independent readings (each lasting for 1 min) were recorded for all three solutions and graphs were plotted with mean of these readings, showing the activation kinetics of the electroceutical fabric in response to these wetting solutions. Data are mean ± SEM.

Figure 3: Physical characterization of the purified coronavirus. (**A**) SEM image of purified respiratory CoV. (**B**) Viral particle number in the purified respiratory CoV sample was quantified using NTA. An estimated yield of $4x10^8$ viruses with one major peak corresponding to 100 nm size, was obtained from the adopted viral purification protocol. (**C – F**) Zeta potential readouts of four independent (mean ± SEM shown) purified coronavirus sample preparation and the different attributes of analyses are depicted. (**C**) Individual zeta potential values of purified respiratory CoV

suspended in 18.2 MΩ water. (**D**) Zeta potential distribution within individual reads. (**E**) Individual phase plots determined by applying alternating voltage and reaching minimum between 1.75 – 2.00 s. (**F**) Electrokinetic observation obtained by measuring mobility of the virus in response to an external electrical field.

Figure 4: Zeta potential and nanosight tracking analysis of the purified coronavirus following contact with and retrieval from the electroceutical fabric. (**A**) Absolute quantification of viral particles recovered from the fabric after treatment with f_e. A two-fold and four-fold reduction in the recovered viral number was observed after 1 and 5 min treatment, respectively. (**B**) Schematic diagram showing the recovery of viral particles from fabric and the subsequent experiments that were performed. (**C**) Viral particle number was quantified using NTA. One hundred microliters of the purified CoV was spotted on 1.5 cm discs of electroceutical fabric and recovered using incomplete EMEM, after 1 or 5 min of contact with the fabric. (**D-F)** Changes in viral zeta potential and affiliated parameters after contact with the fabric for 1 min or 5 min. Data are mean ± SEM.

Figure 5: Eradication of respiratory coronavirus infectivity upon contact with the electroceutical fabric. ST cells were infected with respiratory CoV (4×10^4 viruses). In other test sets, the virus (10^5) was brought in contact with the fabric for either 1 min or 5 min. After 7 days of infection, cells were observed for cytopathic effects (CPE, rounding and sloughing) by phase contrast microscopy. Host cell viability was objectively quantified using dual staining with Calcein AM (green, viable) and PI (red, non-viable). (**A**) uninfected ST cells (u); (**B**) ST cells infected with virus (CoV, 4×10^4); (**C**) ST cells infected with viruses pre-exposed to the sham fabric (f_s1 and f_s5); and (**D**) ST cells infected with viruses pre-exposed to the electroceutical fabric for 1 or 5 minutes, respectively (f_e1 and f_e5). ST cells infected with untreated virus or f_s-contacted virus

showed distinct signs of CPE and loss of cell viability. Cells infected virus which were subjected to contact with the electroceutical fabric for 1 (f_e1) or 5 (f_e5) minute did not display any further loss of cell viability above and beyond the basal level of cell death expected at that phase of the life-cycle of the cell. (**E**) Quantitative plotting of changes in cell viability as determined by PI/calcein expressed as fold-change over the basal cell death level expected as part of standard cell culture process. (**F**) Changes in cell viability as determined by the MTT (3-(4,5-dimethylthiazol-2-yl)-2,5-diphenyltetrazolium bromide) assay. Scale bars in images represent 100µm. Phase contrast images were captured at 40X magnification. Corresponding zoom out images showing a larger field of view were taken at 20X and presented as Figure S2. Data are mean ± SEM.

Figure 6: Lentiviral infectivity in response to contact with the electroceutical fabric. (**A**) HEK293 cells were infected with 4 x 10^4 Lentivirus CSCGW *mut6*. In other test sets, the virus was brought in contact with the fabric for either 1 min (f_s1 or f_e1) or 5 min (f_s5 or f_e5). Recovered viral particles (4 x 10^4) were counted and used to treat cells at MOI of 10. After 96 h of infection, HEK293 cells were microscopically assessed for the expression of GFP which would be an endpoint of successful infection. (**B**) Data are mean ± SEM.

Appendix Figure

Figure S1: The prototype face mask utilizing stretchable electroceutical textile. (**A**) Photomicrograph of the region cut from the face mask and used for SEM and EDX analysis. (**B** and **C**) SEM and EDX analysis for silver and zinc deposition on the textile. Regions of mask used for EDX analysis have been marked and annotated in the respective figure panel.

Figure S2: Phase contrast microscopy images of ST cells, uninfected or infected with CoV (either treated with f_s or f_e for 1 min or 5 min). These images are taken at 20X magnification displaying a larger field of view. Zoom-in images (40X) shown Figure 5. Scale bars, 100 µm.

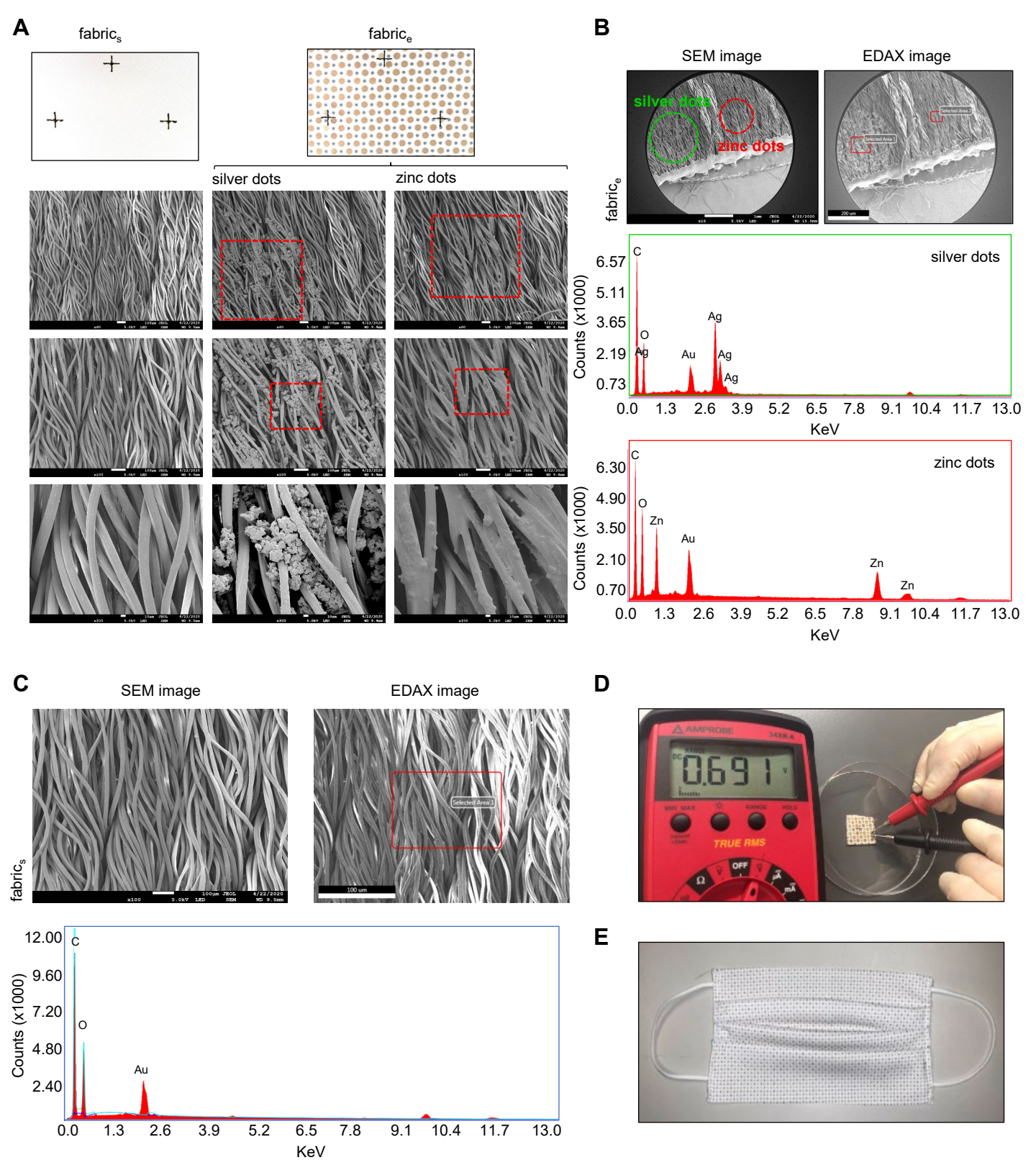
A
fabric$_s$
fabric$_e$
silver dots
zinc dots
B
SEM image
EDAX image
silver dots
zinc dots
fabric$_e$
silver dots
Counts (x1000)
6.57
5.11
3.65
2.19
0.73
C
O
Ag
Au
Ag
Ag
Ag
0.0 1.3 2.6 3.9 5.2 6.5 7.8 9.1 10.4 11.7 13.0
KeV
zinc dots
Counts (x1000)
6.30
4.90
3.50
2.10
0.70
C
O
Zn
Au
Zn
Zn
0.0 1.3 2.6 3.9 5.2 6.5 7.8 9.1 10.4 11.7 13.0
KeV
C
SEM image
EDAX image
fabric$_s$
Selected Area 1
100 um
12.00
9.60
7.20
4.80
2.40
Counts (x1000)
C
O
Au
0.0 1.3 2.6 3.9 5.2 6.5 7.8 9.1 10.4 11.7 13.0
KeV
D
AMPROBE
0.691
TRUE RMS
OFF
E

Figure 1

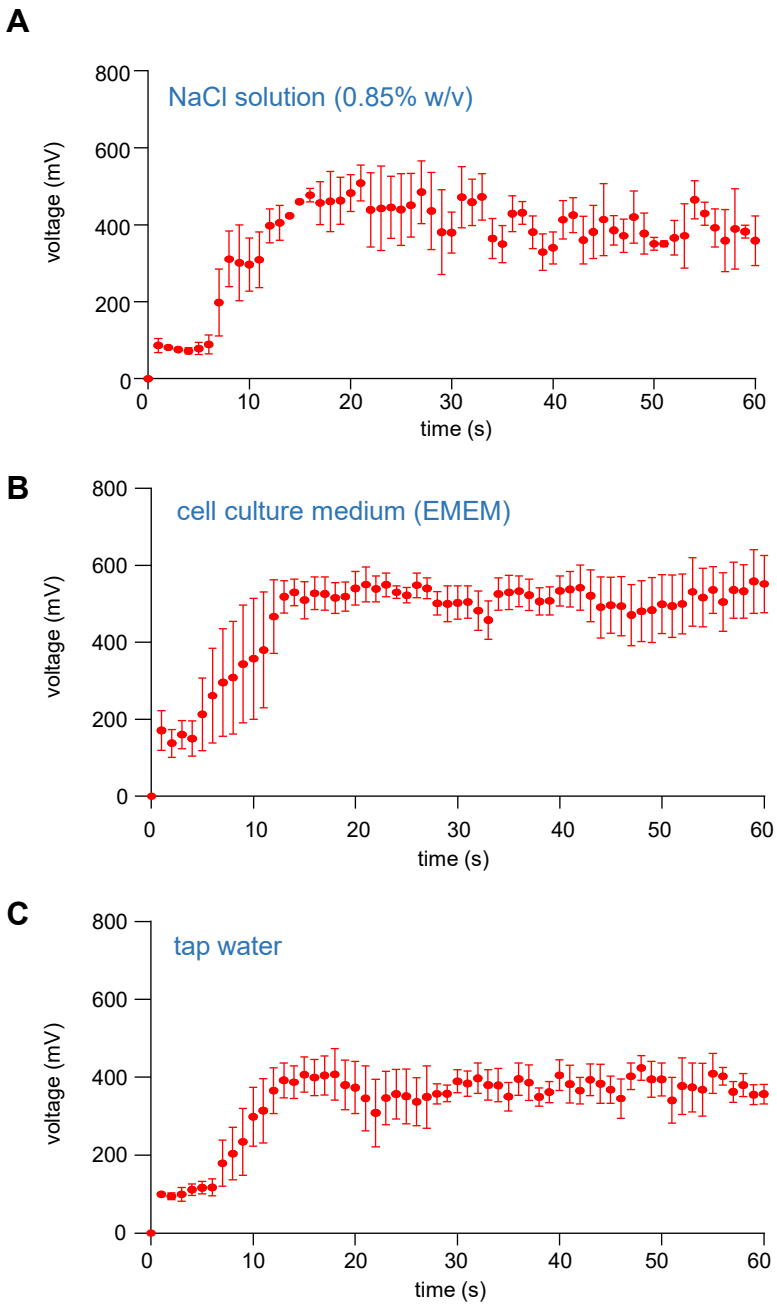
A
NaCl solution (0.85% w/v)
voltage (mV)
time (s)
B
cell culture medium (EMEM)
voltage (mV)
time (s)
C
tap water
voltage (mV)
time (s)

Figure 2

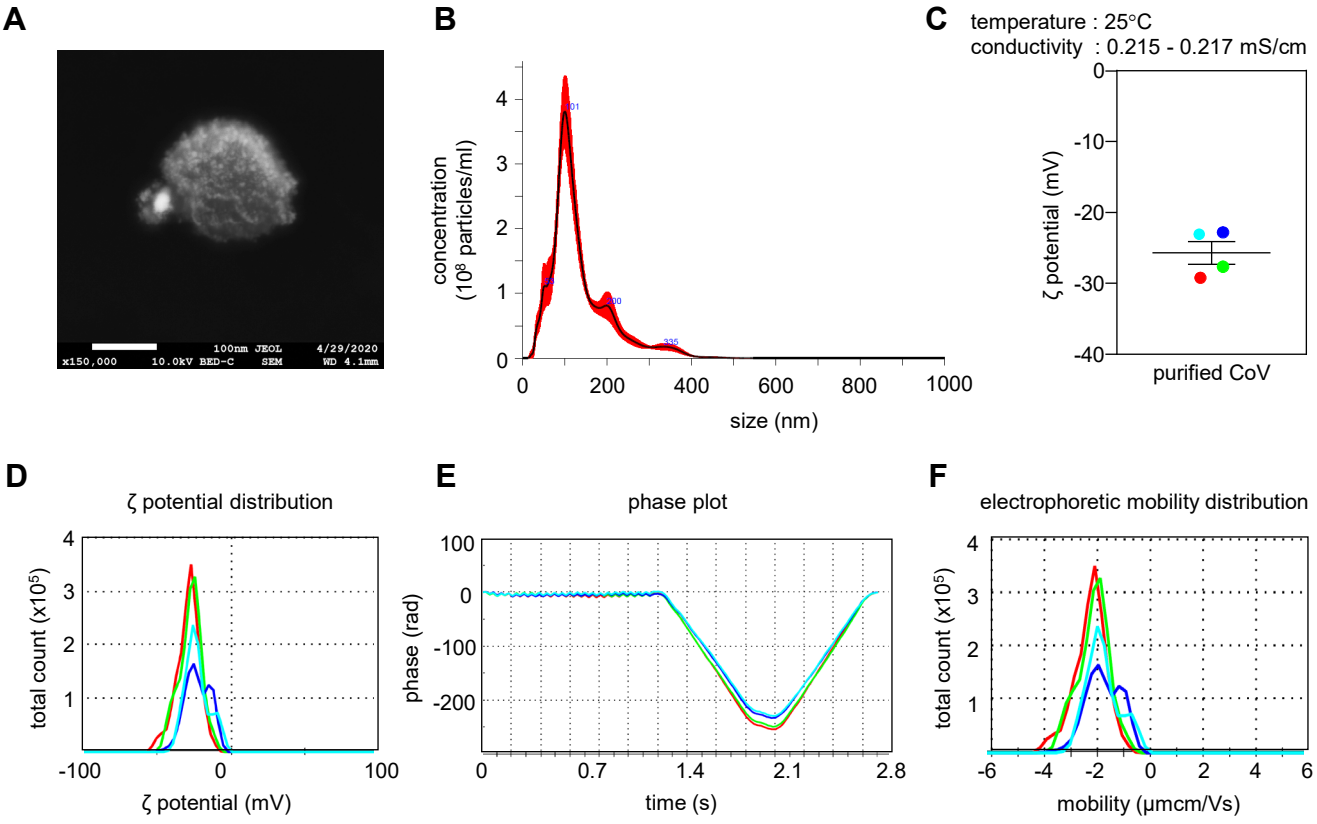
A
100nm JEOL 4/29/2020
x150,000 10.0kV BED-C SEM WD 4.1mm
B
concentration (10^8 particles/ml)
size (nm)
C
temperature : 25°C
conductivity : 0.215 - 0.217 mS/cm
ζ potential (mV)
purified CoV
D
ζ potential distribution
total count (x10^5)
ζ potential (mV)
E
phase plot
phase (rad)
time (s)
F
electrophoretic mobility distribution
total count (x10^5)
mobility (μmcm/Vs)

Figure 3

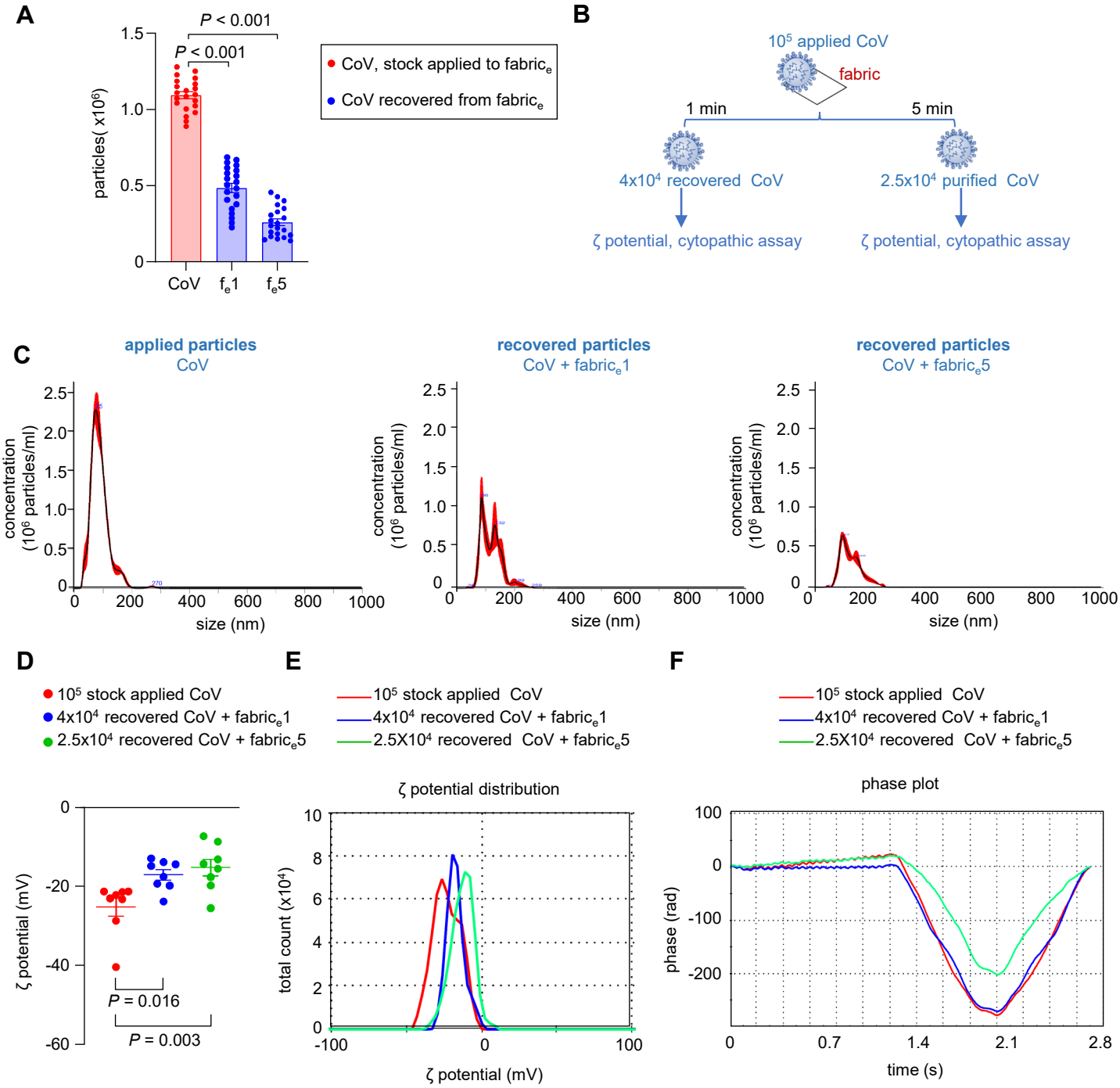
A
P < 0.001
P < 0.001
particles(x10^6)
CoV
f_e1
f_e5
CoV, stock applied to fabric_e
CoV recovered from fabric_e
B
10^5 applied CoV
fabric
1 min
5 min
4x10^4 recovered CoV
2.5x10^4 purified CoV
ζ potential, cytopathic assay
ζ potential, cytopathic assay
C
applied particles
CoV
recovered particles
CoV + fabric_e1
recovered particles
CoV + fabric_e5
concentration (10^6 particles/ml)
size (nm)
D
10^5 stock applied CoV
4x10^4 recovered CoV + fabric_e1
2.5x10^4 recovered CoV + fabric_e5
ζ potential (mV)
P = 0.016
P = 0.003
E
10^5 stock applied CoV
4x10^4 recovered CoV + fabric_e1
2.5X10^4 recovered CoV + fabric_e5
ζ potential distribution
total count (x10^4)
ζ potential (mV)
F
10^5 stock applied CoV
4x10^4 recovered CoV + fabric_e1
2.5X10^4 recovered CoV + fabric_e5
phase plot
phase (rad)
time (s)

Figure 4

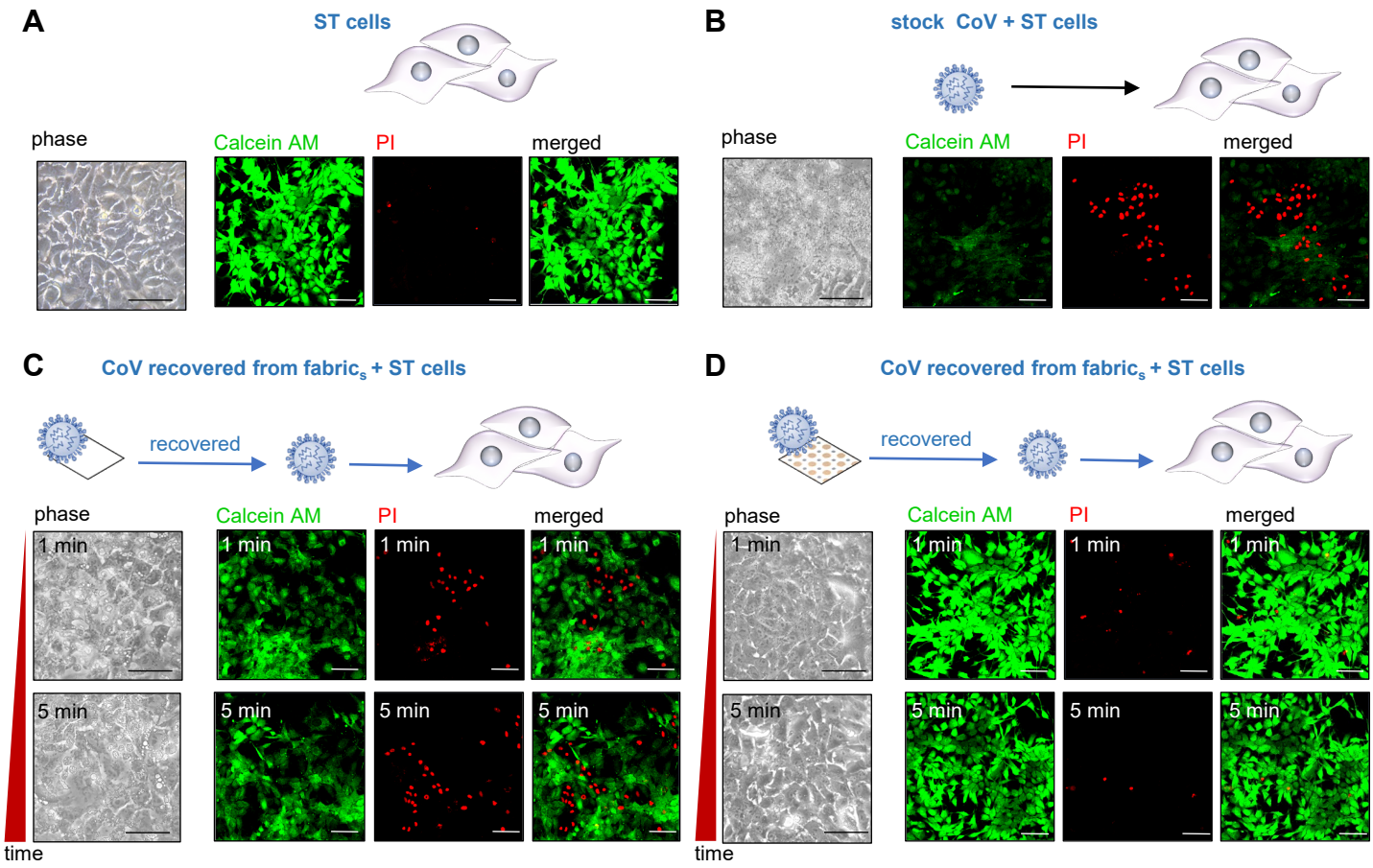

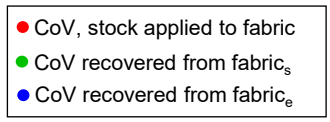

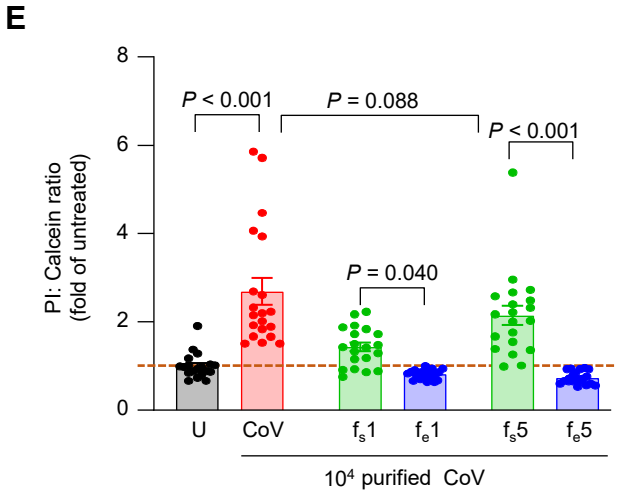

basal death of cells in culture

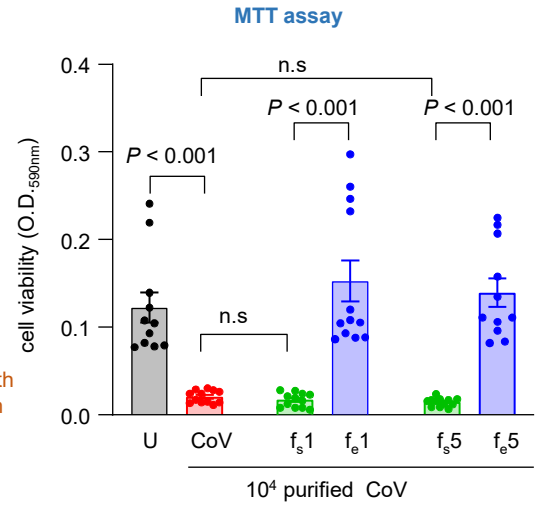

Figure 5

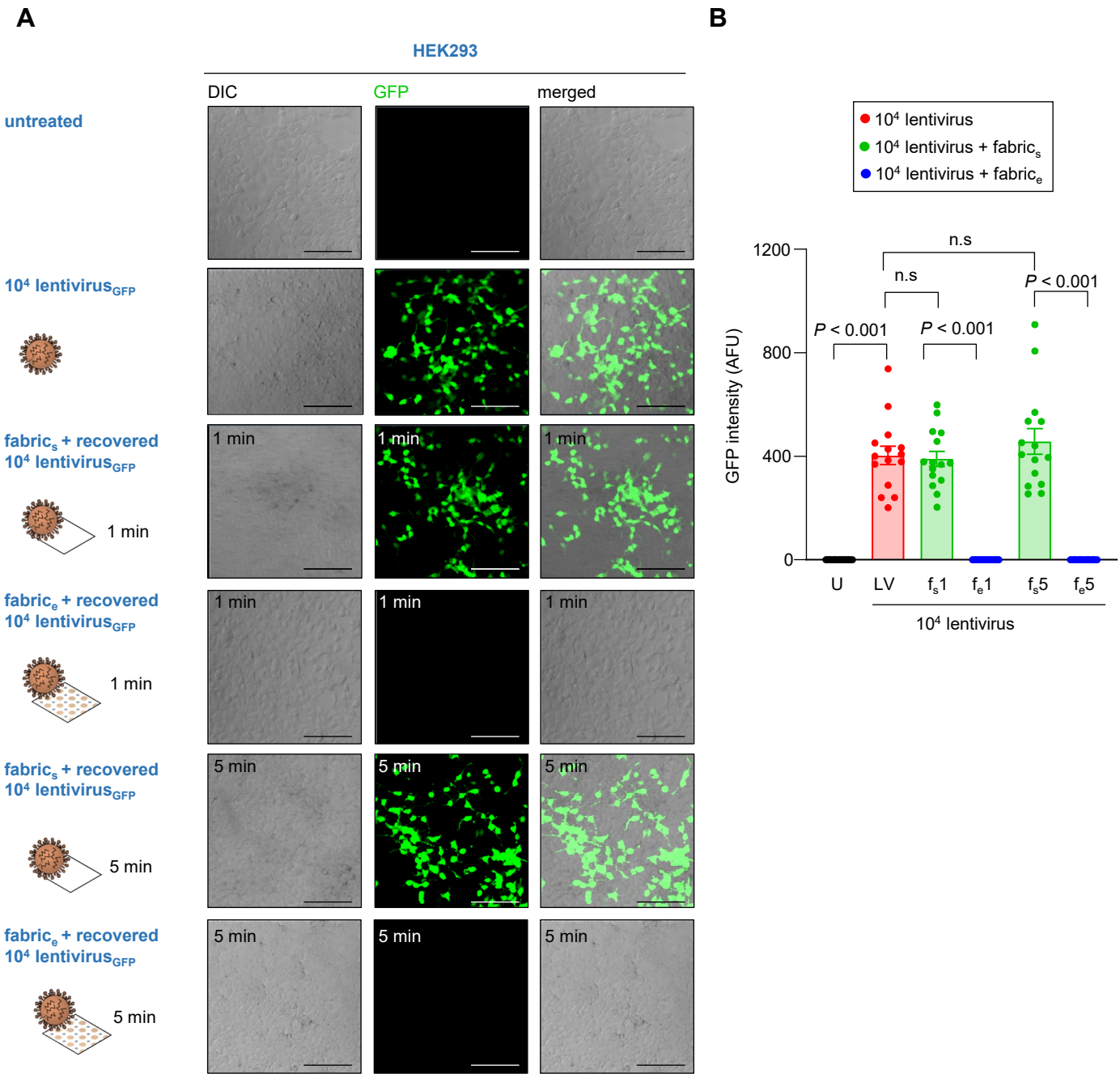
A
HEK293
DIC
GFP
merged
untreated
10⁴ lentivirus_GFP
fabric_s + recovered 10⁴ lentivirus_GFP
1 min
fabric_e + recovered 10⁴ lentivirus_GFP
1 min
fabric_s + recovered 10⁴ lentivirus_GFP
5 min
fabric_e + recovered 10⁴ lentivirus_GFP
5 min
B
10⁴ lentivirus
10⁴ lentivirus + fabric_s
10⁴ lentivirus + fabric_e
GFP intensity (AFU)
1200
800
400
0
n.s
n.s
P < 0.001
P < 0.001
P < 0.001
U
LV
f_s1
f_e1
f_s5
f_e5
10⁴ lentivirus

Figure 6

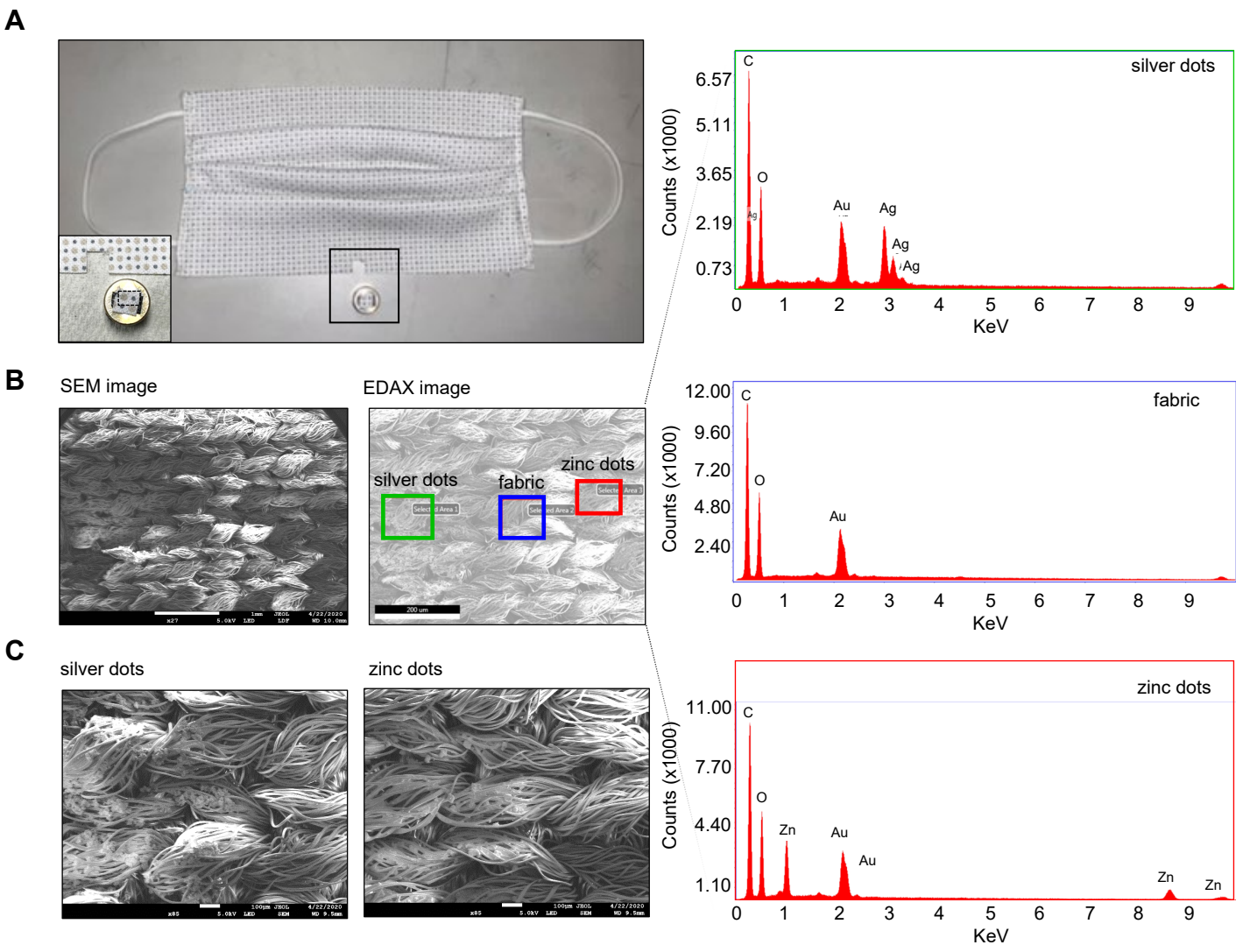
A
B
C
SEM image
EDAX image
silver dots
fabric
zinc dots
silver dots
zinc dots
Counts (x1000)
KeV
C
O
Au
Ag
Zn

Figure S1

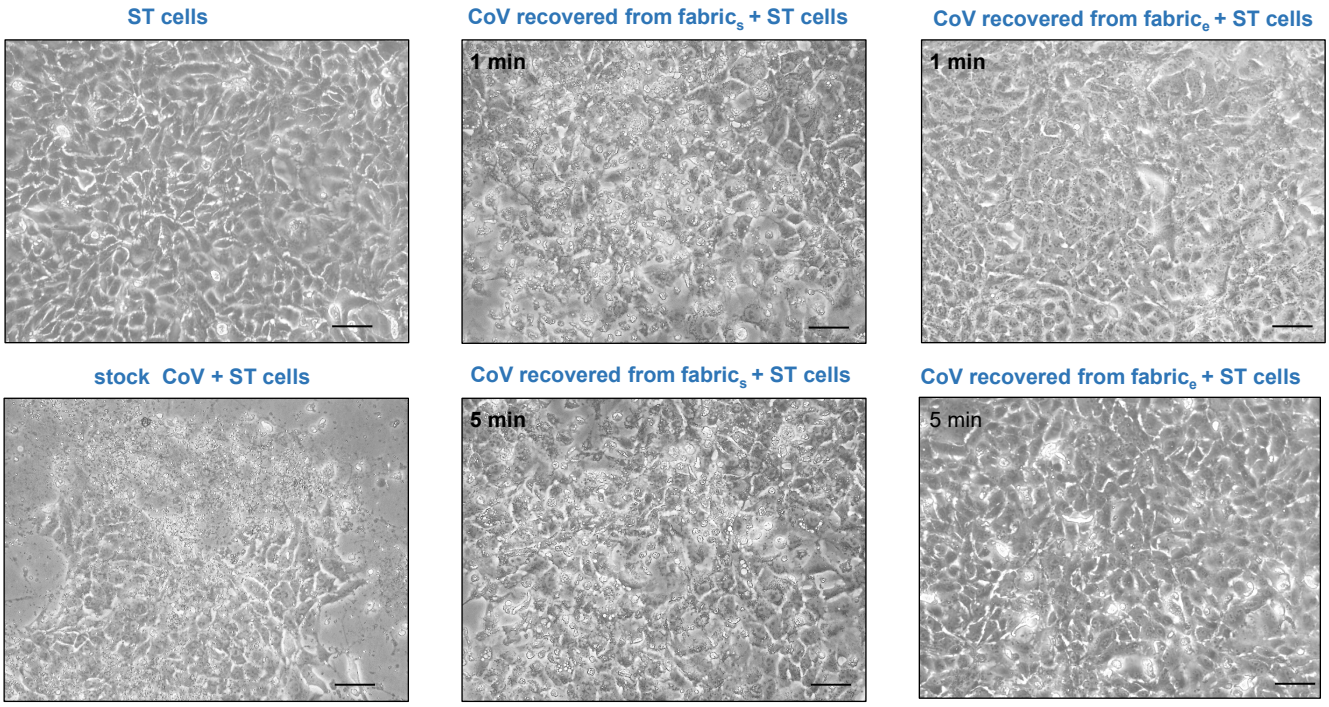
ST cells
CoV recovered from fabric$_s$ + ST cells
1 min
CoV recovered from fabric$_e$ + ST cells
1 min
stock CoV + ST cells
CoV recovered from fabric$_s$ + ST cells
5 min
CoV recovered from fabric$_e$ + ST cells
5 min

Figure S2